

Degenerate Plaquette Physics as Key Ingredient of HTSC in cuprates

Mikhail Katsnelson

In collaboration with

Alexander Lichtenstein (Hamburg)

Based on the papers (many thanks to all the coauthors):

PHYSICAL REVIEW B **94**, 125133 (2016)

Plaquette valence bond theory of high-temperature superconductivity

Malte Harland

Institut für Theoretische Physik, Universität Hamburg, Jungiusstraße 9, 20355 Hamburg, Germany

Mikhail I. Katsnelson

Radboud University, Institute for Molecules and Materials, Heyendaalseweg 135, 6525AJ Nijmegen, The Netherlands

Alexander I. Lichtenstein

*The Hamburg Centre for Ultrafast Imaging, Luruper Chaussee 149, Hamburg 22761, Germany
and Institut für Theoretische Physik, Universität Hamburg, Jungiusstraße 9, 20355 Hamburg, Germany*

(Received 10 April 2016; revised manuscript received 26 July 2016; published 19 September 2016)

PHYSICAL REVIEW B **100**, 024510 (2019)

Josephson lattice model for phase fluctuations of local pairs in copper oxide superconductors


Malte Harland,¹ Sergey Brener,¹ Alexander I. Lichtenstein,¹ and Mikhail I. Katsnelson²

¹*Institute of Theoretical Physics, University of Hamburg, Jungiusstraße 9, 20355 Hamburg, Germany*

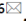
²*Institute for Molecules and Materials, Radboud University, 6525AJ, Nijmegen, The Netherlands*

PHYSICAL REVIEW B **101**, 045119 (2020)

Exactly solvable model of strongly correlated d -wave superconductivity

Malte Harland ¹, Sergey Brener,^{1,2} Mikhail I. Katsnelson,³ and Alexander I. Lichtenstein^{1,2}

Detecting quantum critical points in the t - t' Fermi-Hubbard model via complex network theory

Andrey A. Bagrov^{1,2,3,6} , Mikhail Danilov^{4,6}, Sergey Brener^{4,5}, Malte Harland⁴,
Alexander I. Lichtenstein^{3,4,5} & Mikhail I. Katsnelson^{2,3}

Scientific Reports | (2020) 10:20470

Degenerate plaquette physics as key ingredient of high-temperature superconductivity in cuprates

Michael Danilov¹, Erik G. C. P. van Loon ^{2,3,4}, Sergey Brener^{1,5}, Sergei Isakov⁶, Mikhail I. Katsnelson ⁷ and
Alexander I. Lichtenstein ^{1,5} 

npj Quantum Materials (2022)7:50

35 years of HTSC in cuprates

J. Bednorz and K. Müller Z. Phys. B 64, 189 (1986)

“Possible highTc superconductivity in the Ba–La–Cu–O system”
Tc=30 K

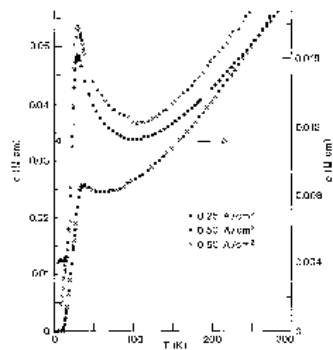
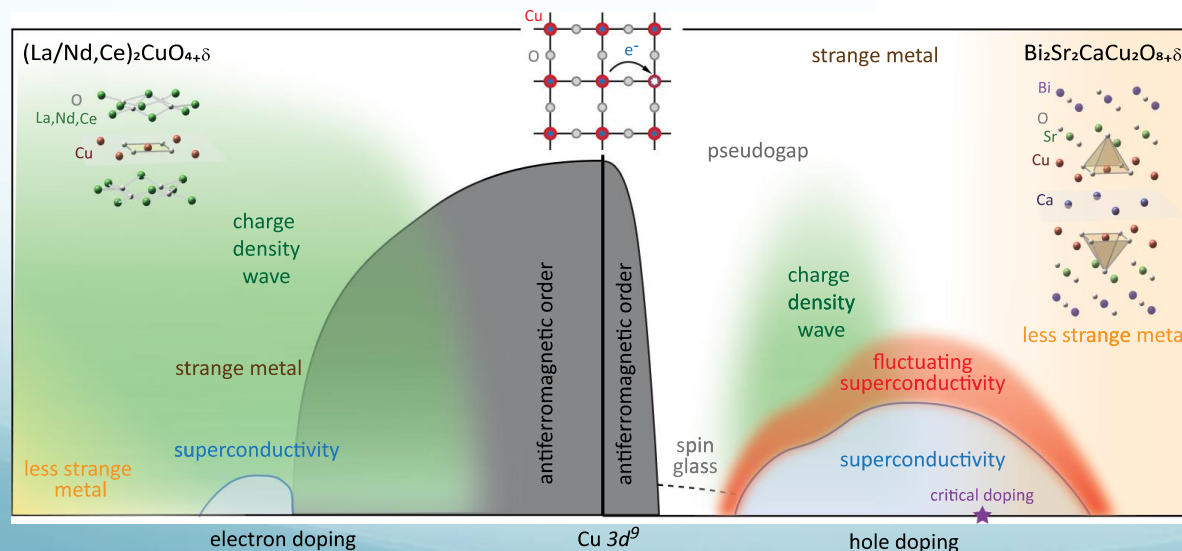
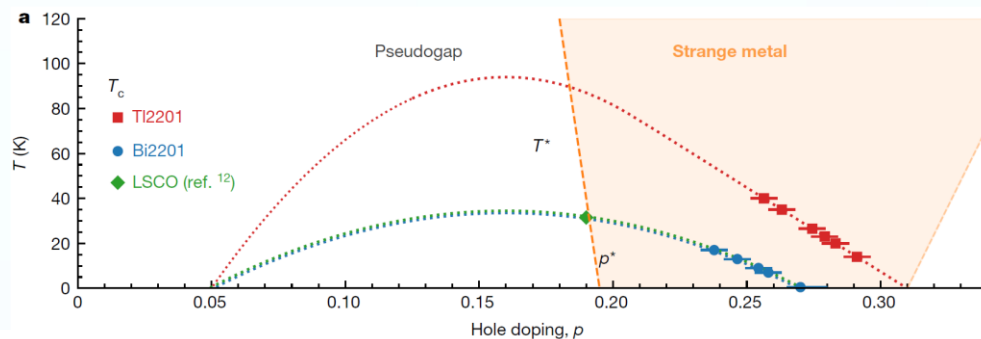


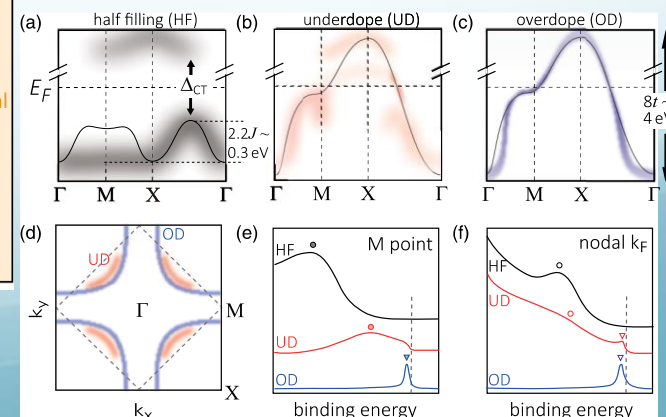
Fig. 1. Temperature dependence of resistivity ρ and Hall coefficient R_H for samples with $x(\text{Bi}) = 1$ (upper curves) and $x(\text{Bi}) = 0.55$ (lower curves). Right axis: The last two cases show the influence of carrier density.

Transport data

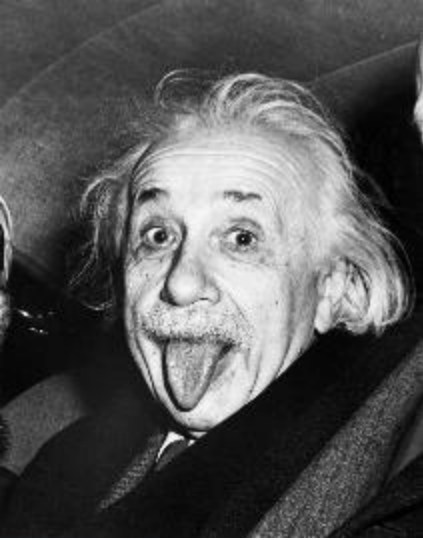
J. Ayres et al, Nature 595, 661 (2021)



ARPES and other spectroscopy



J. Sobota et al, RMP 93, 025006 (2021)



Epigraphs

Make things as simple as possible but not simpler (A. Einstein)



Local moments and localized states

P. W. Anderson

Reviews of Modern Physics, Vol. 50, No. 2, April 1978

(Nobel lecture)

shall soon discuss. Very often such a simplified model throws more light on the real workings of nature than any number of *ab initio* calculations of individual situations, which even where correct often contain so much detail as to conceal rather than reveal reality. It can be a disadvantage rather than an advantage to be able to compute or to measure too accurately, since often what one measures or computes is irrelevant in terms of mechanism. After all, the perfect computation simply reproduces Nature, it does not explain her.

Cuprates are complicated

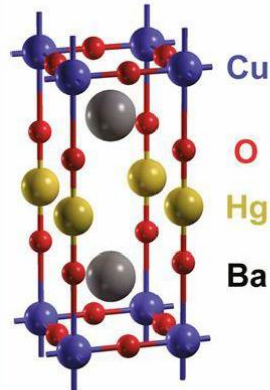
Apical oxygen?
Interlayer hopping?

...
Phonons?
(Bi)polarons?
Anharmonicities?

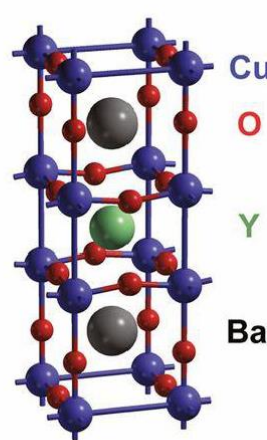
...
Spin fluctuations as glue?
Charge density waves?

...

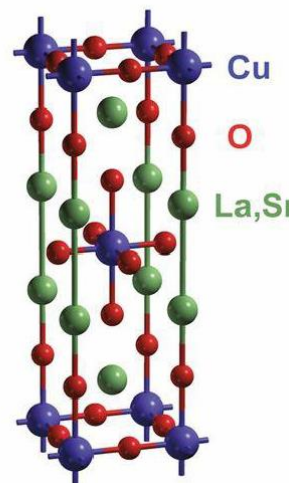
$\text{HgBa}_2\text{CuO}_{4+\delta}$
(Hg1201)



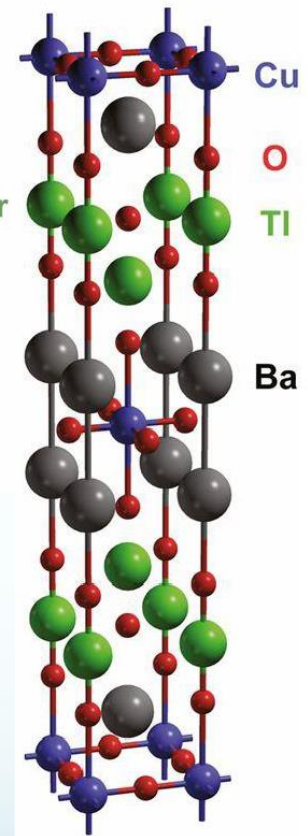
$\text{YBa}_2\text{Cu}_3\text{O}_{6+\delta}$
(YBCO)



$\text{La}_{2-x}\text{Sr}_x\text{CuO}_4$
(LSCO)

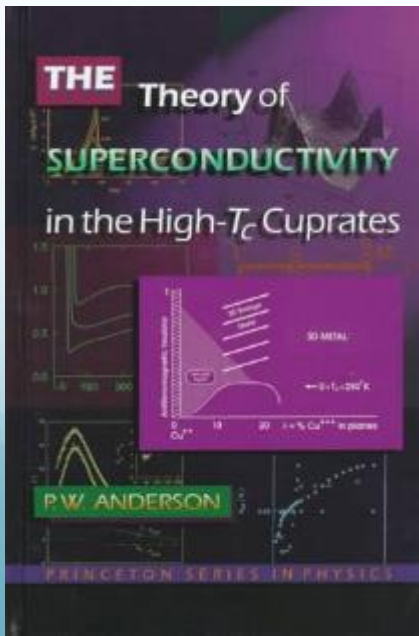


$\text{Ti}_2\text{Ba}_2\text{CuO}_{6+\delta}$
(TI2201)



Hypothesis: Basic physics can be described within a single-band Hubbard model

Very nontrivial and we still do not know whether this is true or not



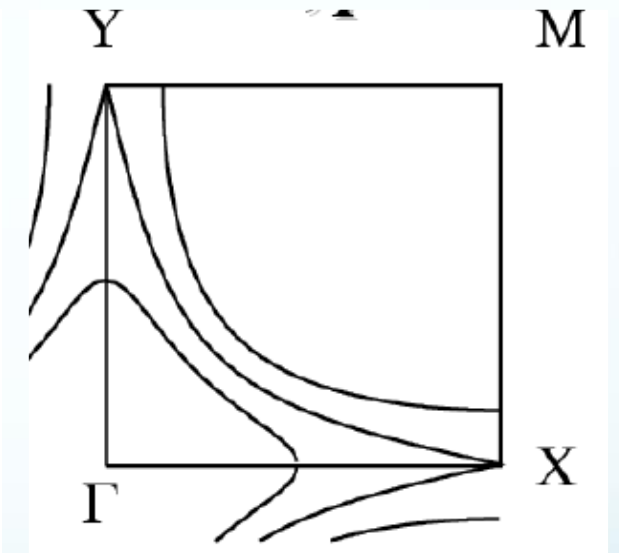
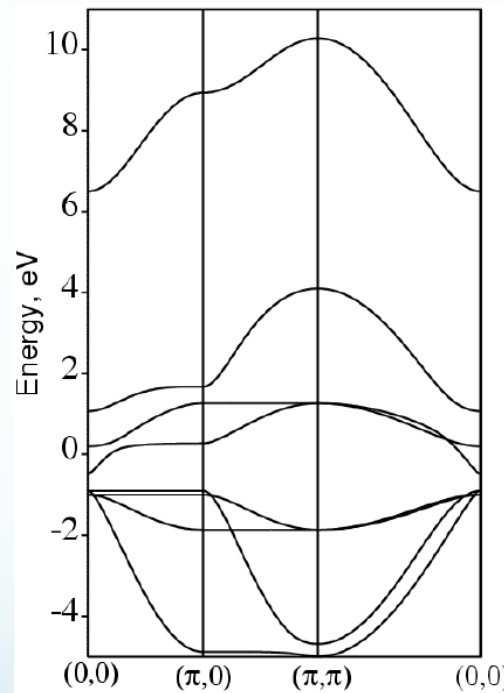
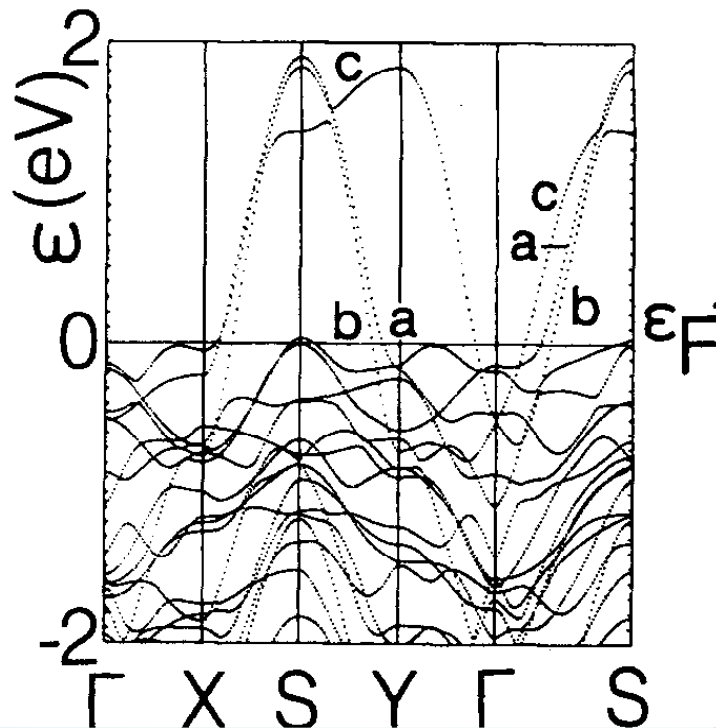
Mapping of electronic structure

LDA ENERGY BANDS, LOW-ENERGY HAMILTONIANS, t' , t'' , $t_{\perp}(\mathbf{k})$, and J_{\perp}

O. K. ANDERSEN, A. I. LIECHTENSTEIN, O. JEPSEN and F. PAULSEN

Max-Planck Institut für Festkörperforschung, D-70569 Stuttgart, Germany

J. Phys. Chem. Solids Vol. 56, No. 12, pp. 1573–1591, 1995



Minimal single-band model

This band is of quite complicated orbitals,
p-d hybridization is inside them

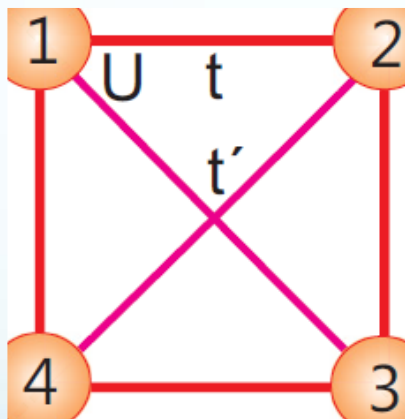
LDA electronic structure of YBCO

Mapping of electronic structure II

$$H = -t \sum_{\langle i,j \rangle, \sigma} c_{i,\sigma}^\dagger c_{j,\sigma} - t' \sum_{\langle\langle l,k \rangle\rangle, \sigma} c_{l,\sigma}^\dagger c_{k,\sigma} + U \sum_i n_{i,\uparrow} n_{i,\downarrow}$$

the pairs $\langle i, j \rangle$ of nearest neighbors

the pairs $\langle\langle l, k \rangle\rangle$ of next-to-nearest (diagonal) neighbors



t - t' Hubbard model

Band-Structure Trend in Hole-Doped Cuprates and Correlation with T_c max

E. Pavarini, I. Dasgupta,* T. Saha-Dasgupta,† O. Jepsen, and O. K. Andersen

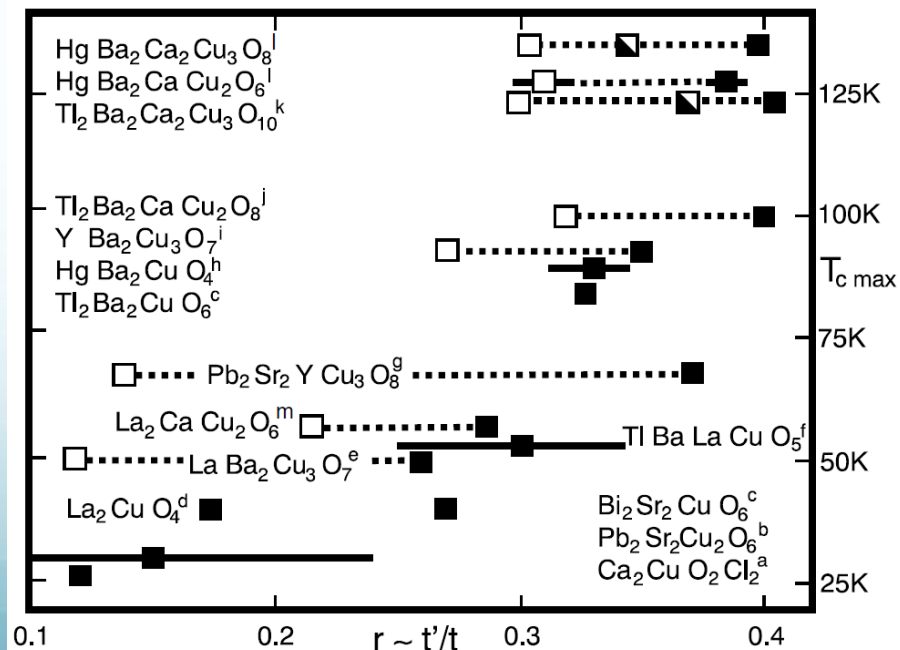
VOLUME 87, NUMBER 4

PHYSICAL REVIEW LETTERS

23 JULY 2001

Empirically: t' is useful for high T_c

Existing theories mostly ignores this
(How accurate is the mapping? How adequate is the model? Etc. etc.)



Weak-coupling regime: Van Hove scenario

Coincidence of saddle points with Fermi energy in 2D results in inapplicability of Fermi liquid theory due to divergences of vertex parts (I. E. Dzialoshinskii 1987)

PHYSICAL REVIEW B, VOLUME 64, 165107

Effects of van Hove singularities on magnetism and superconductivity in the t - t' Hubbard model: A parquet approach

V. Yu. Irkhin, A. A. Katanin, and M. I. Katsnelson
Institute of Metal Physics, 620219 Ekaterinburg, Russia
(Received 1 March 2001; published 3 October 2001)

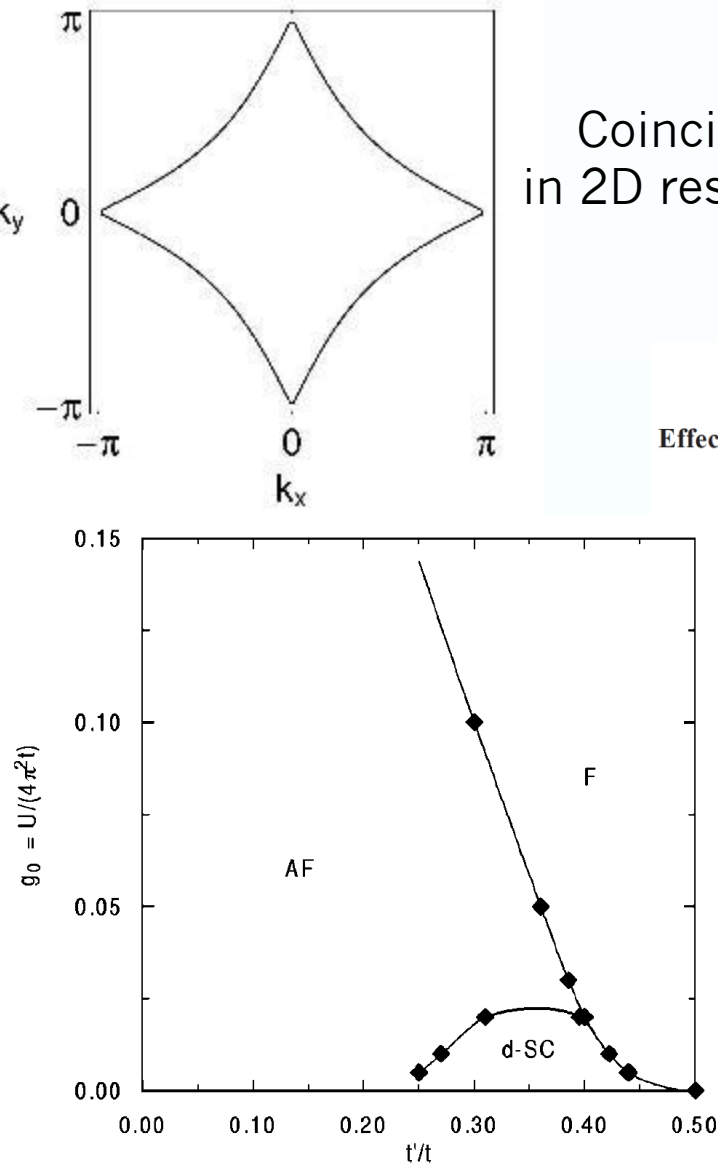


FIG. 9. The phase diagram from parquet equations for van Hove filling ($\mu=0$) in g_0 - t'/t coordinates.

Parquet approximation should be valid for small enough dimensionless coupling constant and predicts existence of SC dome; the role of t' is crucial (without it one has exact nesting and totally different divergences)

Weak-coupling regime: Van Hove scenario II

Not a theory for just one point: flat band formation and pinning of VHS to the Fermi energy

VOLUME 89, NUMBER 7

PHYSICAL REVIEW LETTERS

12 AUGUST 2002

Robustness of the Van Hove Scenario for High- T_c Superconductors

V. Yu. Irkhin, A. A. Katanin, and M. I. Katsnelson

Due to huge quasiparticle damping

$$\delta\rho(\varepsilon) \simeq \frac{k_c^2}{\pi|\varepsilon|} \frac{C \ln(\Lambda t/|\varepsilon|)}{[1 + C \ln^2(\Lambda t/|\varepsilon|)]^2}$$

Pinning of the chemical potential to VHS

$$\tilde{\mu}(n) = \Lambda t \exp(-\text{const}/|n - n_{\text{VH}}|^{1/2})$$

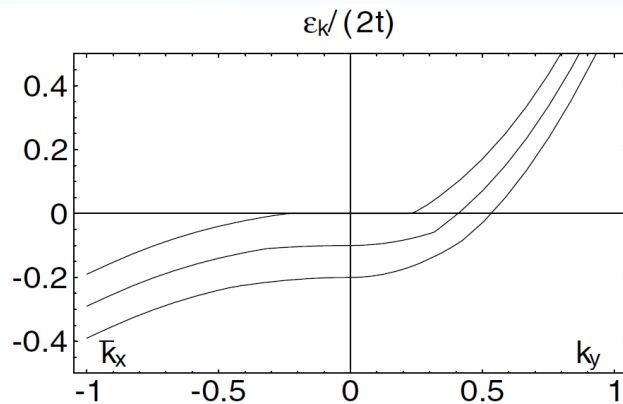


FIG. 1. Quasiparticle dispersion for $t'/t = -0.3$ and $U = 4t$ from RG approach. The values of the chemical potential are $\tilde{\mu} = 0, -0.2t, -0.4t$ (from top to bottom).

Strong and moderate coupling: Cluster DMFT approach

PHYSICAL REVIEW B

VOLUME 62, NUMBER 14

1 OCTOBER 2000-II

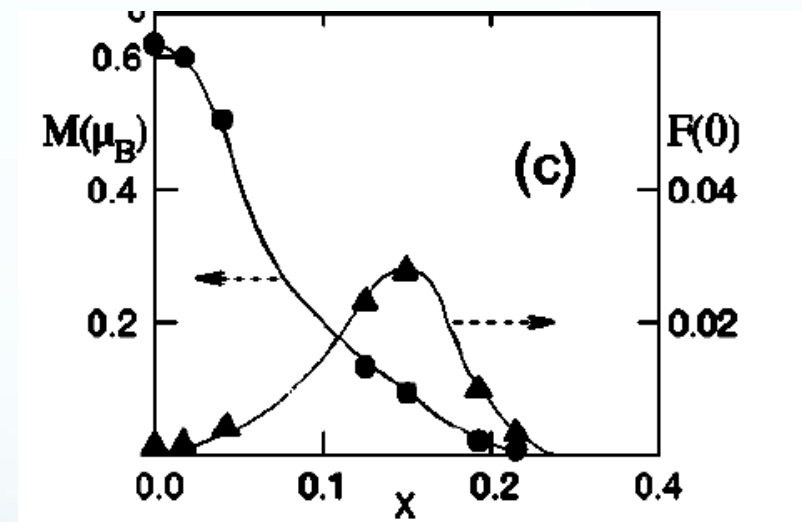
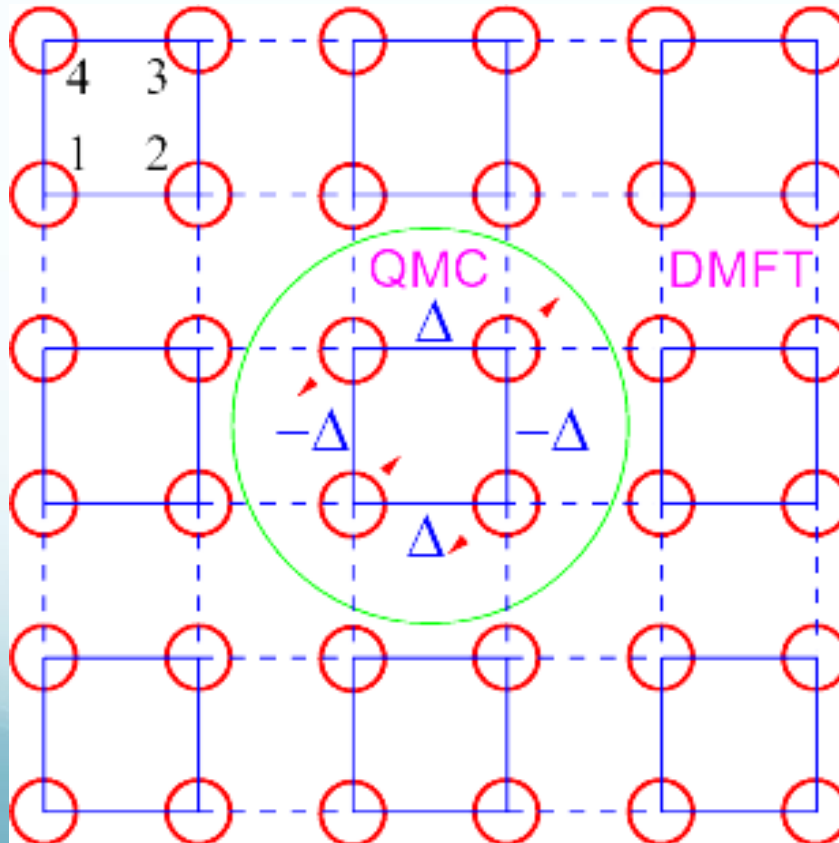
Antiferromagnetism and *d*-wave superconductivity in cuprates: A cluster dynamical mean-field theory

A. I. Lichtenstein¹ and M. I. Katsnelson²

LSCO parameter

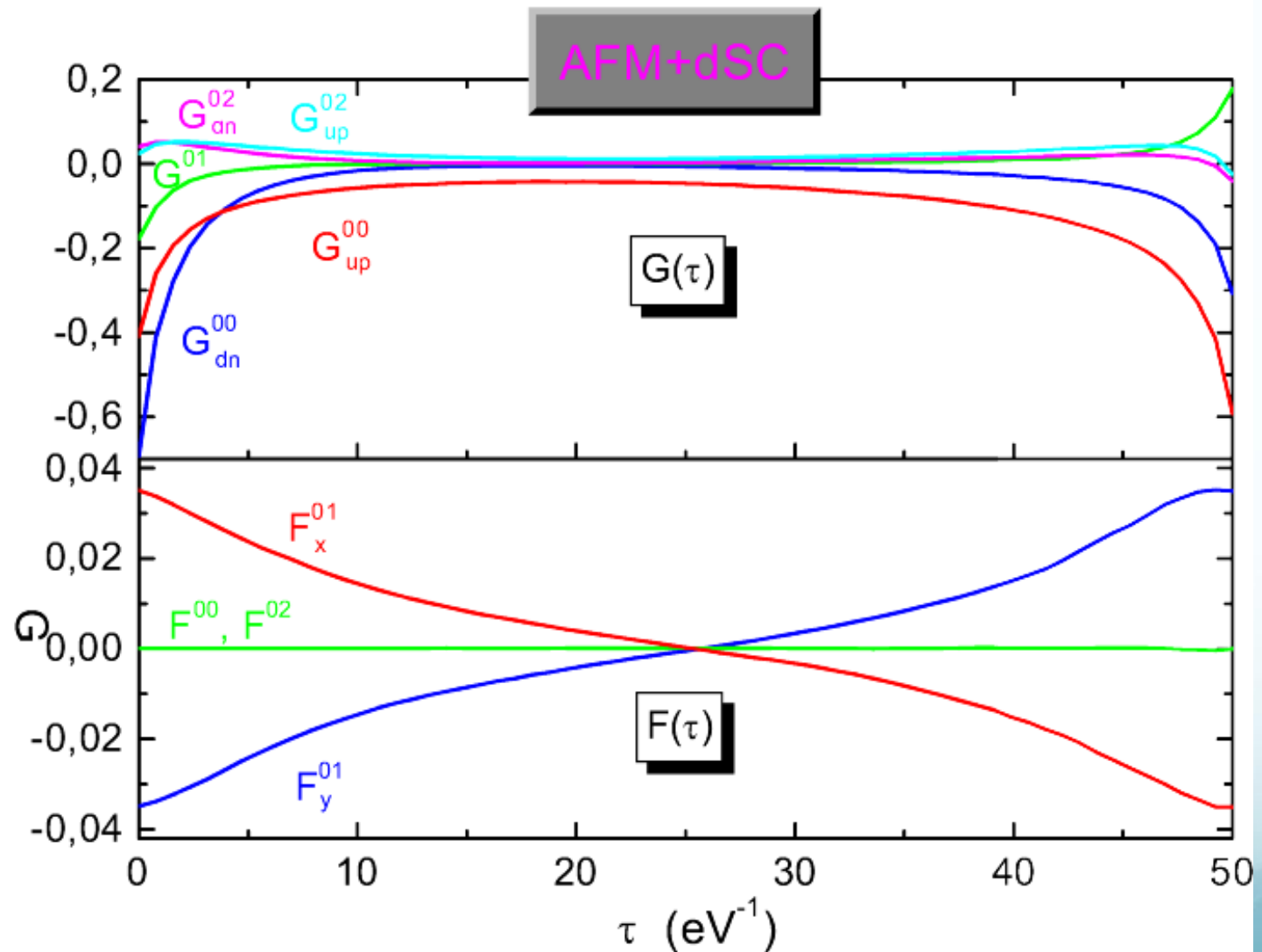
$$t'/t = -0.15$$

$$U/W = 0.6$$



Coexistence of superconducting (F) and AFM (M) ordering but AFM can be short-range

Cluster DMFT approach II



Local plaquette physics

Huge number of calculations, two versions: DCA (M. Jarrell) with coarse-graining in k-space and cluster DMFT in real space

Can we separate some most important specific features?

Probably, **yes! – Accidental (?) degeneracy of plaquette ground states**

M. Harland, MIK, A. Lichtenstein, Phys. Rev. B 94, 125133 (2016)

Start with isolated plaquette

$$H_p = \sum_{(i,j)=1\dots 4} h_{ij}^0 c_{i\sigma}^\dagger c_{j\sigma} + \sum_{i=1\dots 4} U n_{i\uparrow} n_{i\downarrow}$$

$$-\hat{h}_0 = \begin{pmatrix} \mu & t & t' & t \\ t & \mu & t & t' \\ t' & t & \mu & t \\ t & t' & t & \mu \end{pmatrix}.$$

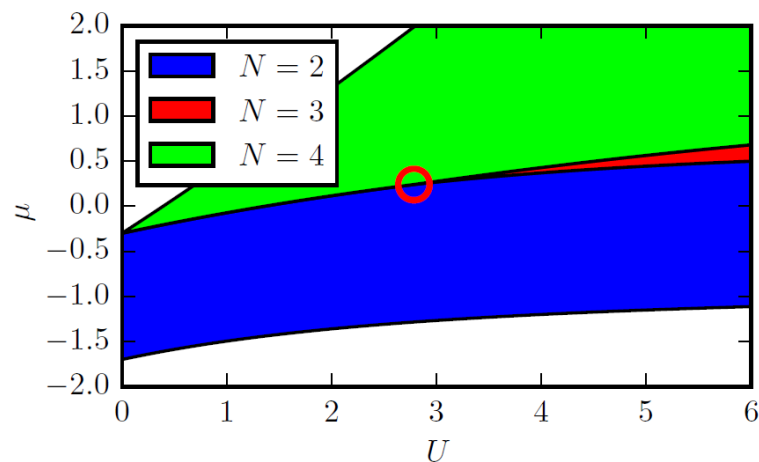


FIG. 1. Zero-temperature phase diagram of the isolated plaquette as a function of the Hubbard U and chemical potential μ in the proximity of the quantum critical point (circle) for $t'/t = -0.3$.

Local plaquette physics II

Plaquette in the bath (hybridization V as parameter)

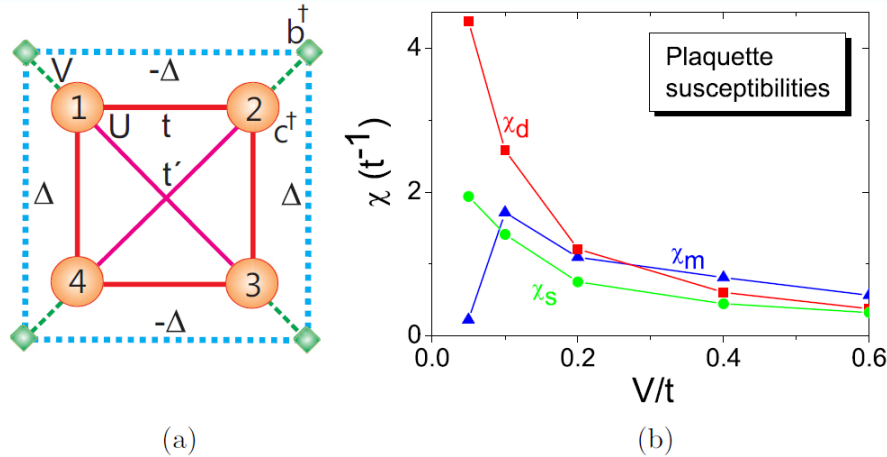


FIG. 2. (a) Sketch of the plaquette in the four-site bath with the $d_{x^2-y^2}$ -wave order parameter. (b) Superconducting (χ_d), singlet bond order (χ_s), and antiferromagnetic (χ_m) susceptibilities of the plaquette in a bath as a function of the hybridization V for $U = 3$ and $\mu = 0.27$.

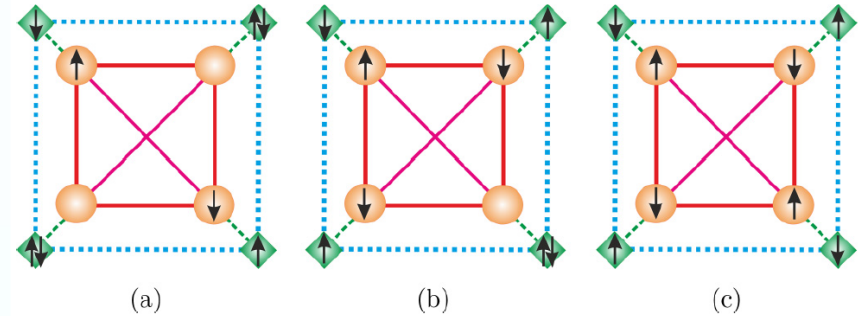


FIG. 3. The main contributions to the plaquette's singlet ground state in a four-site bath with the $d_{x^2-y^2}$ -wave order parameter is the hybridization $V = 0.2\Delta_d = 0.05$ for $U = 3$ and $\mu = 0.27$. (a) Sector $N = 2$ with coefficient = 0.05 and four antisymmetric contributions. (b) Sector $N = 3$ with coefficient = 0.06 and eight antisymmetric contributions. (c) Sector $N = 4$ with coefficient = 0.08 and two antisymmetric contributions.

Observation: when considering singlet ground state with bath, doubles sit on bath sites, effectively we have something like Gutzwiller projector despite U is not very large

Local plaquette physics III

Lehmann representation for single-particle Green function

$$g_{\alpha\beta}(\omega) = \sum_n \frac{\langle \Psi_0^N | c_\alpha | \Psi_n^{N+1} \rangle \langle \Psi_n^{N+1} | c_\beta^\dagger | \Psi_0^N \rangle}{\hbar\omega - (E_n^{N+1} - E_0^N) + i\eta} \mp \sum_k \frac{\langle \Psi_0^N | c_\beta^\dagger | \Psi_k^{N-1} \rangle \langle \Psi_k^{N-1} | c_\alpha | \Psi_0^N \rangle}{\hbar\omega - (E_0^N - E_k^{N-1}) - i\eta}$$

If we have degeneracy of ground states with N and $N \pm 1$ particles we have a pole of Green function near zero frequency (cf. with phenomenology of soft “hidden fermion” by Imada et al, e.g. PRB 82, 134505 (2010)).

When we have lattice of resonances we have pseudogap instead of peaks, cf Anderson (or Kondo) lattices

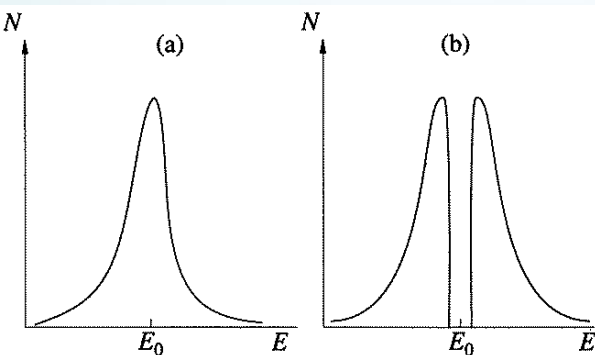


Fig. 6.3. Diagram of the density of electronic states in the hybridization model for (a) an isolated impurity and (b) the lattice.

Avoided level crossing between dispersion and dispersionless states result in (pseudo)gap formation

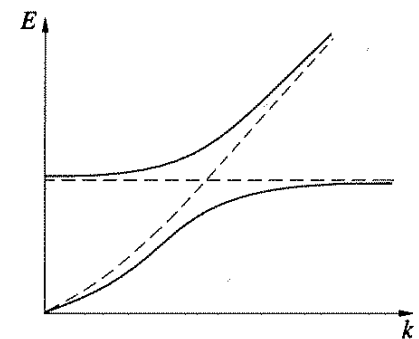


Fig. 6.4. Energy spectrum diagram for the hybridization model.

Local plaquette physics IV

Pseudogap formation at low temperatures
when degenerate plaquette is put into environment

Line (blue) of six-fold degeneracy of the ground state

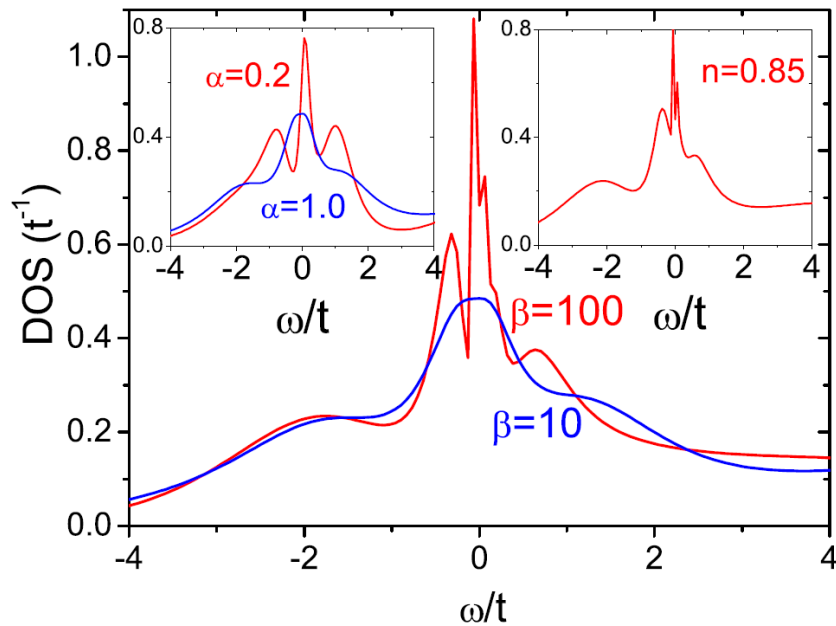
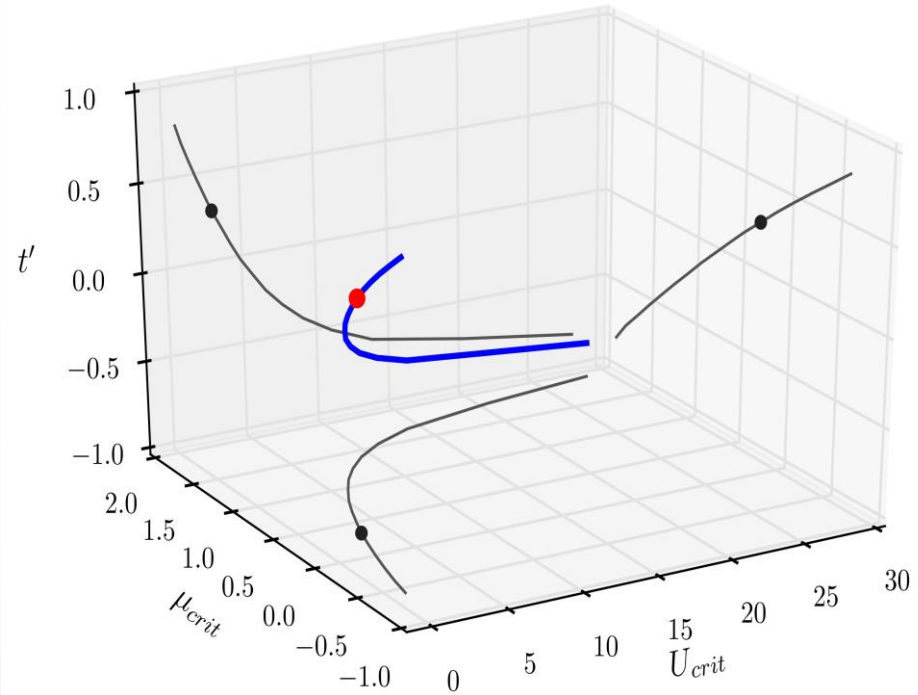


FIG. 5. Density of states for both spins of the plaquette CDMFT for $U = 6$ and $\mu = 0.54$ for different temperatures, (the left inset) with plaquette-lattice hoppings scaled by a factor of α at $\beta = 10$ and (the right inset) for optimal doping $n = 0.85$ at $\beta = 100$.



Malte Harland, PhD thesis, 2016

Quadruple Bethe lattice as exactly solvable model of d-wave SC

M. Harland et al, PRB 101, 045119 (2020)

FIG. 1. Quadruple Bethe lattice, four Bethe lattices (dashed lines) interconnected via plaquettes (solid lines). The coordination number for each Bethe lattice of this figure is set to $z = 3$, and four sites of each Bethe lattice are depicted. An entire Bethe lattice exhibits an infinite number of sites with self-similar structure. Next-nearest-neighbor hoppings of the plaquette are omitted for convenience.

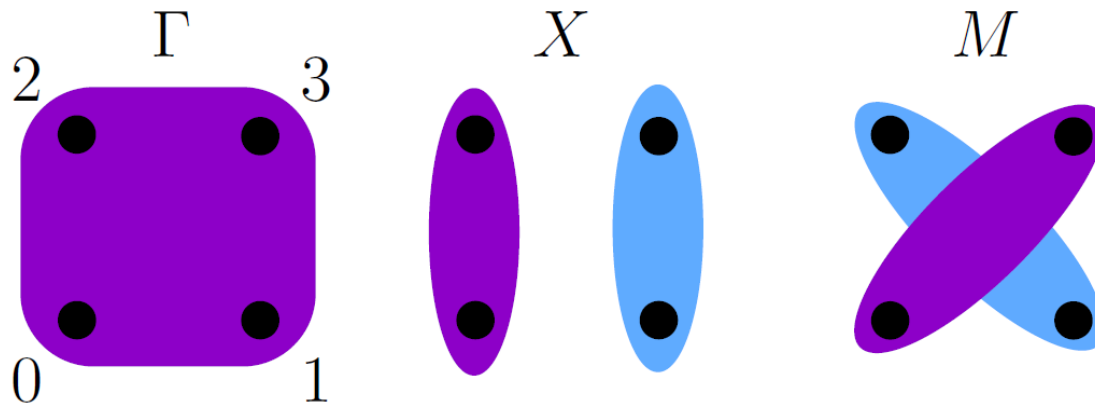
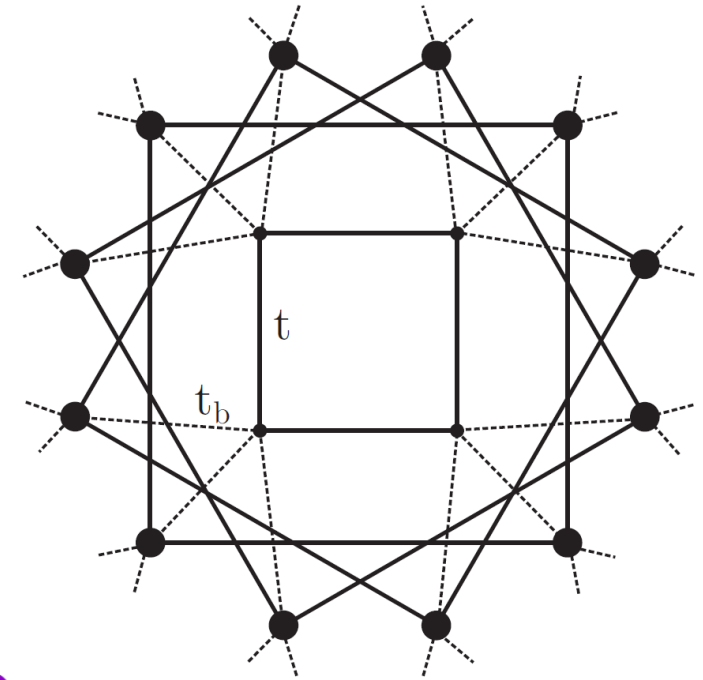


FIG. 2. Illustration of the plaquette orbitals/momenta Γ , X , and M (Y omitted), i.e., the basis that diagonalizes the hopping in plaquette-site space (0, 1, 2, and 3). Colors denote symmetries of the orbitals.

Quadruple Bethe lattice as exactly solvable model of d-wave SC II

Self-consistency condition

$$\Sigma(i\omega_n) = \mathcal{G}^{-1}(i\omega_n) - G^{-1}(i\omega_n)$$

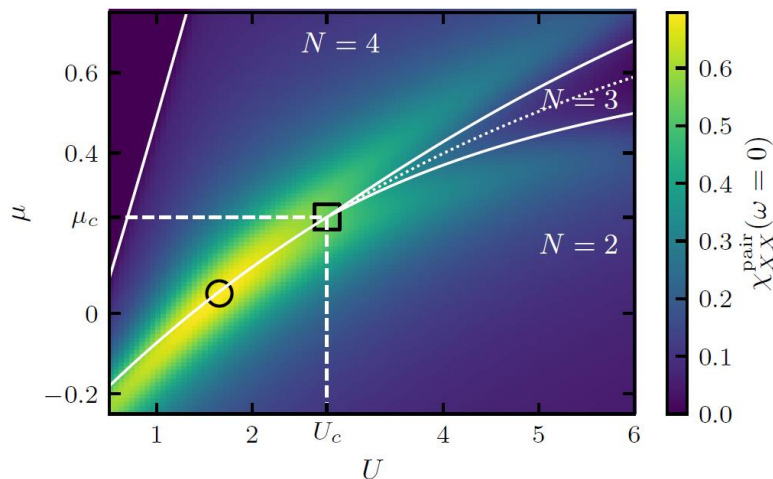
Nambu Green's function, two sublattices A and B to allow AFM

$$G_{BK\sigma, BK'\sigma'}(i\omega_n) = - \sum_{\tau\tau'} R_{\sigma\tau} G_{AK\tau, AK'\tau'}^*(i\omega_n) R_{\tau'\sigma'}^\dagger$$

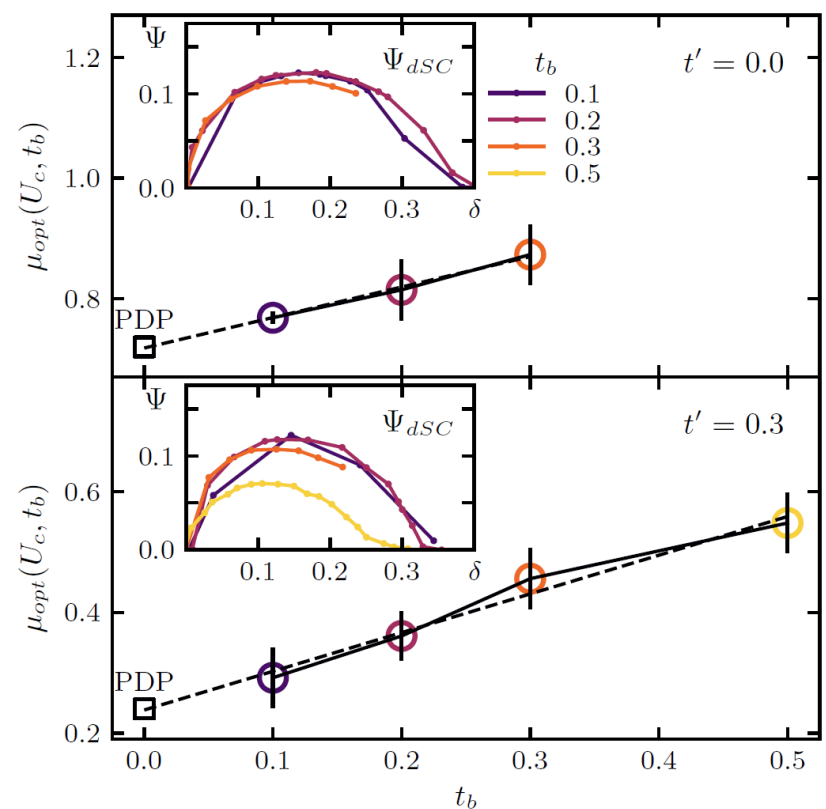
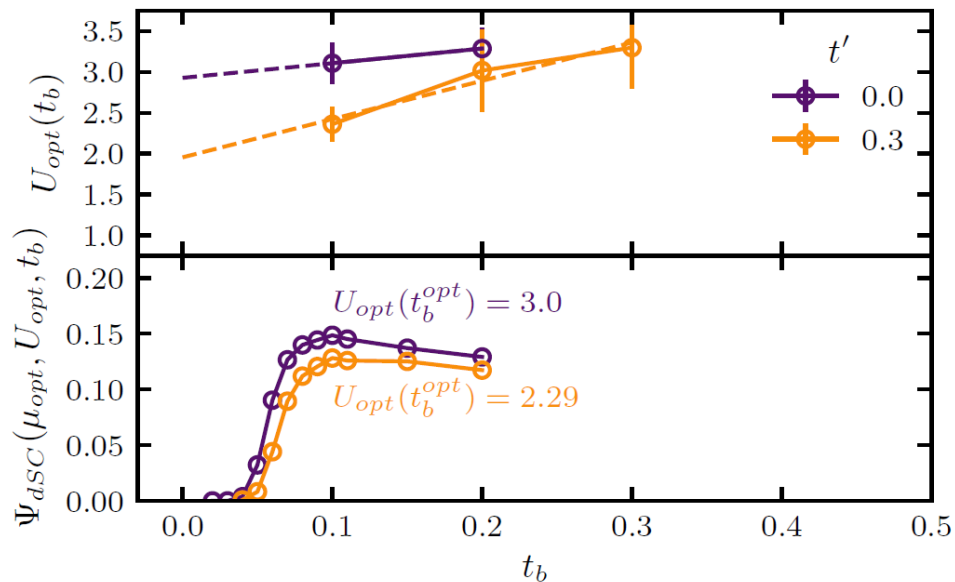
$$R = e^{i\pi\sigma^y/2}$$

$$\begin{aligned} \mathcal{G}_{AK\sigma, AK'\sigma'}^{-1}(i\omega_n) = & i\omega_n \delta_{KK'} \delta_{\sigma\sigma'} + (\mu \delta_{KK'} - t_{KK'}^p) \sigma_{\sigma\sigma'}^z \\ & - t_b^2 \sum_{\tau\tau'} \sigma_{\sigma\tau}^z G_{BK\tau, BK'\tau'}(i\omega_n) \sigma_{\tau'\sigma'}^z. \end{aligned}$$

Quadruple Bethe lattice as exactly solvable model of d-wave SC III



Pair susceptibility for isolated plaquette



Optimal chemical potential for d-wave SC, at $U = U_c$

Optimal U for optimal doping and d-wave SC order parameter

Quadruple Bethe lattice as exactly solvable model of d-wave SC IV

Very rich phase diagram with different types of ordering including spin-triplet superconductivity

$$\begin{aligned}\Psi_{dSC} &= \frac{1}{4^2} \sum_{RR'} (\cos[X(R - R')] - \cos[Y(R - R')]) \\ &\quad \times \langle c_{R\uparrow} c_{R'\downarrow} - c_{R\downarrow} c_{R'\uparrow} \rangle, \\ \Psi_{AFM} &= \frac{1}{4} \sum_R e^{iMR} \langle S_R^z \rangle, \quad \Psi_{PAFM} = \frac{1}{4} \sum_R e^{i\Gamma R} \langle S_R^z \rangle, \\ \Psi_{\pi SC} &= \frac{1}{4^2} \sum_{RR'} (\cos[X(R - R')] - \cos[Y(R - R')]) \\ &\quad \times e^{iMR'} \langle c_{R\uparrow} c_{R'\downarrow} + c_{R\downarrow} c_{R'\uparrow} \rangle.\end{aligned}$$

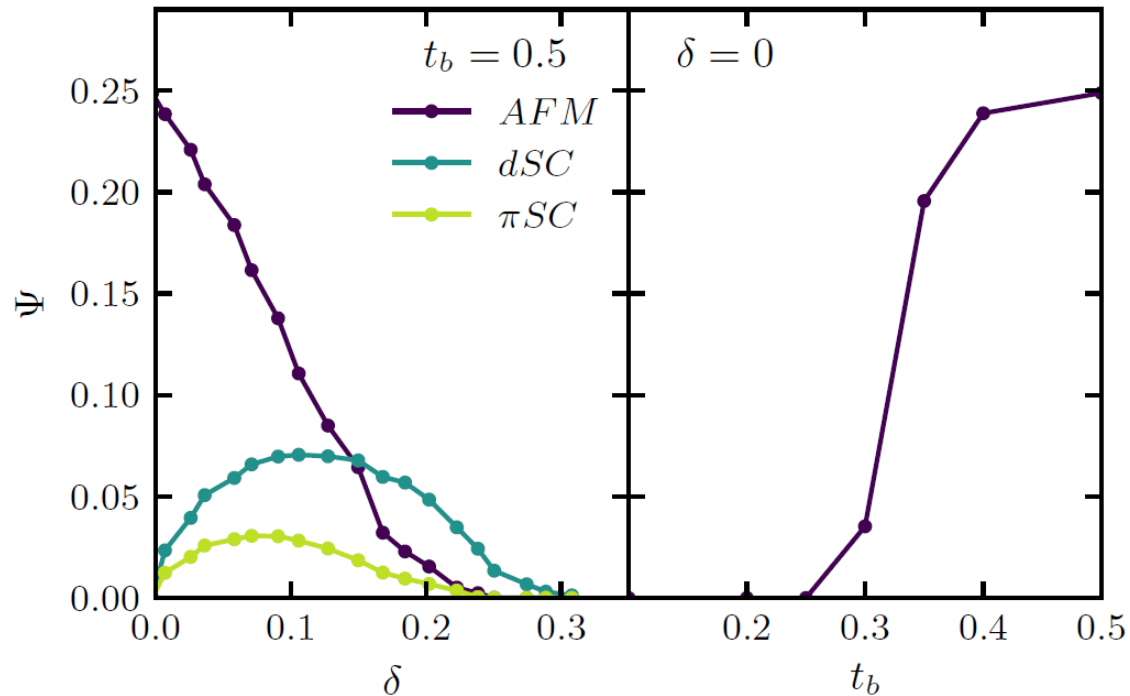


FIG. 17. Order parameters Ψ of antiferromagnetism (AFM), d -wave superconductivity (dSC) and spin-triplet superconductivity (π SC) dependent on hole doping δ for Bethe hopping $t_b = 0.5$ (left) and dependent on t_b for half-filling $\delta = 0$ (right) ($U = 2.78$, $t' = 0.3$).

Quadruple Bethe lattice as exactly solvable model of d-wave SC IV

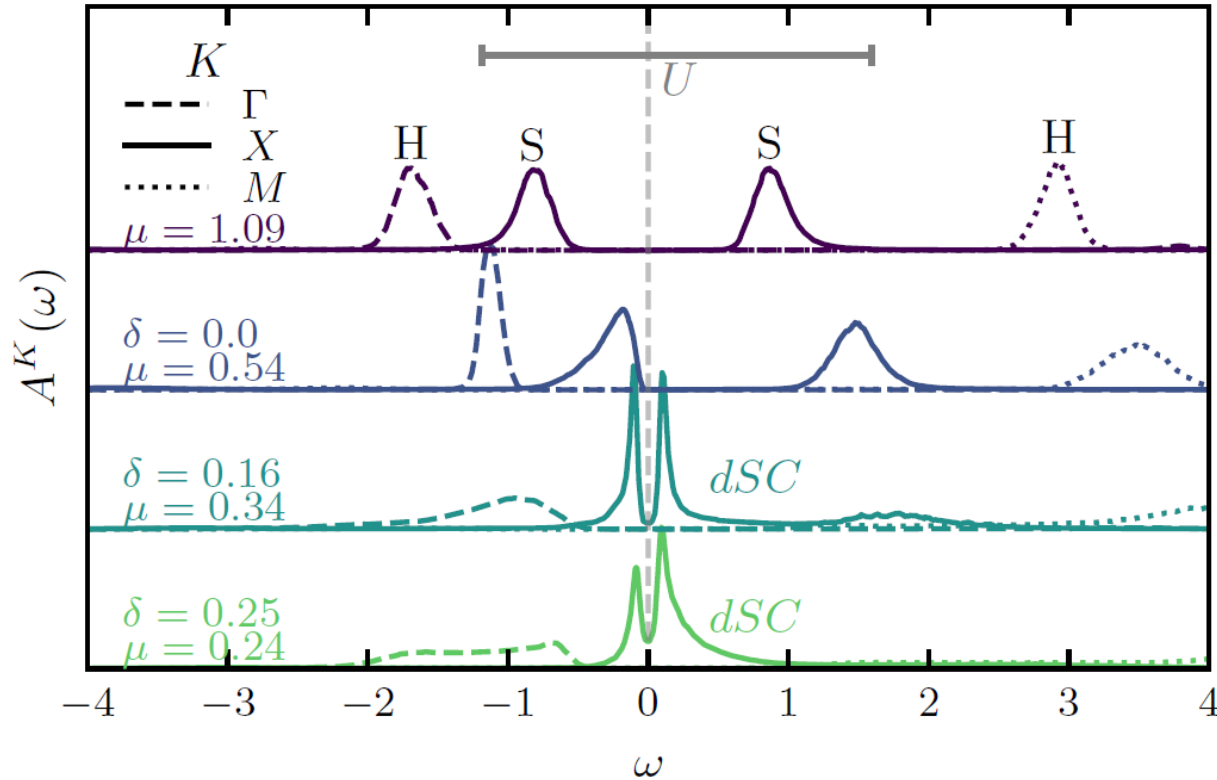


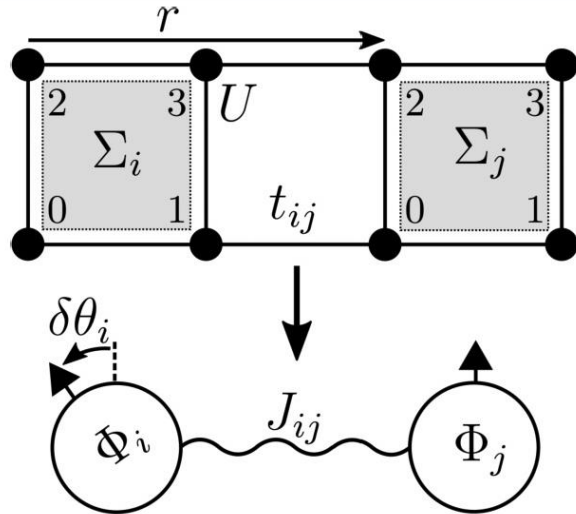
FIG. 14. Momentum resolved spectral function $A^K(\omega)$ for different dopings δ (corresponding to chemical potentials μ) showing a four-peak structure at half-filling ($\delta = 0$) of Hubbard (H) and Slater (S) peaks and for hole-dopings δ the d -wave superconducting gap ($t' = 0.3$, $t_b = 0.2$, and $U = 2.78$). The analytic continuation is obtained by the stochastic optimization method [58–60].

Effective Josephson parameters and superfluid density

M. Harland et al, PRB 100, 024520 (2019)

Borrowed from magnetism: mapping to effective Heisenberg model via small rotations of spins ('magnetic force theorem'); applicable when local moments are well defined

(Lichtenstein, MIK, Gubanov 1984;1985; Lichtenstein, MIK, Antropov,Gubanov, 1987; MIK & Lichtenstein, 2000)



$$\begin{pmatrix} G^{p\uparrow} & F \\ F & G^{h\downarrow} \end{pmatrix}_{ij}^{-1} = \begin{pmatrix} G_0^{p\uparrow} & 0 \\ 0 & G_0^{h\downarrow} \end{pmatrix}_{ij}^{-1} - \delta_{ij} \begin{pmatrix} \Sigma^{p\uparrow} & S \\ S & \Sigma^{h\downarrow} \end{pmatrix}_i$$

Change of local phases in the plaquette

$$\begin{aligned} \delta^* \Sigma_i &= e^{i\delta\theta_i \sigma_z/2} \Sigma_i e^{-i\delta\theta_i \sigma_z/2} - \Sigma_i \\ &\simeq \begin{pmatrix} 0 & (i\delta\theta_i - \frac{(\delta\theta_i)^2}{2}) S_i \\ (-i\delta\theta_i - \frac{(\delta\theta_i)^2}{2}) S_i & 0 \end{pmatrix} \end{aligned}$$

Effective Josephson parameters and superfluid density II

Luttinger-Ward functional

$$\begin{aligned}\Omega &= \Omega_{sp} - \Omega_{dc}, \\ \Omega_{sp} &= -\text{Tr} \ln(-G^{-1}), \\ \Omega_{dc} &= \text{Tr} \Sigma G - \Phi,\end{aligned}$$

Variation according to local force theorem
(Lichtenstein & MIK PRB 2000)

$$\delta\Omega \simeq \sum_{ij} \text{Tr} \left(\delta_{ij} G_{ii} \delta^* \Sigma_i + \frac{1}{2} G_{ij} \delta^* \Sigma_j G_{ji} \delta^* \Sigma_i \right)$$

where δ^* denotes the local variation of the self-energy Σ without taking into account its variation due to the CDMFT self-consistency

Mapping to Josephson lattice Hamiltonian

$$H_{\text{eff}} = - \sum_{ij} J_{ij} \cos(\theta_i - \theta_j)$$

$$J_{ij} = T \text{Tr}_{\omega\alpha} \left(-G_{ij}^{p\uparrow} S_j G_{ji}^{h\downarrow} S_i + F_{ij} S_j F_{ji} S_i \right)$$

Superfluid density

$$H_{\text{eff}} = \frac{1}{2} \sum_{ab} I_{ab} \int d^d r \frac{\partial \theta}{\partial r_a} \frac{\partial \theta}{\partial r_b}$$

$$\begin{aligned}I_{ab} &= \frac{T}{(2\pi)^d} \int d^d k \text{Tr}_{\omega\alpha} \\ &\times \left(-\frac{\partial G^{p\uparrow}(k)}{\partial k_a} S \frac{\partial G^{h\downarrow}(k)}{\partial k_b} S + \frac{\partial F(k)}{\partial k_a} S \frac{\partial F(k)}{\partial k_b} S \right)\end{aligned}$$

Effective Josephson parameters and superfluid density III

$$|t| = 0.35 \text{ eV} \quad U = 8|t| \quad t'/t = -0.3 \quad t_{\perp}/t = 0.15 \quad \text{YBCO}$$

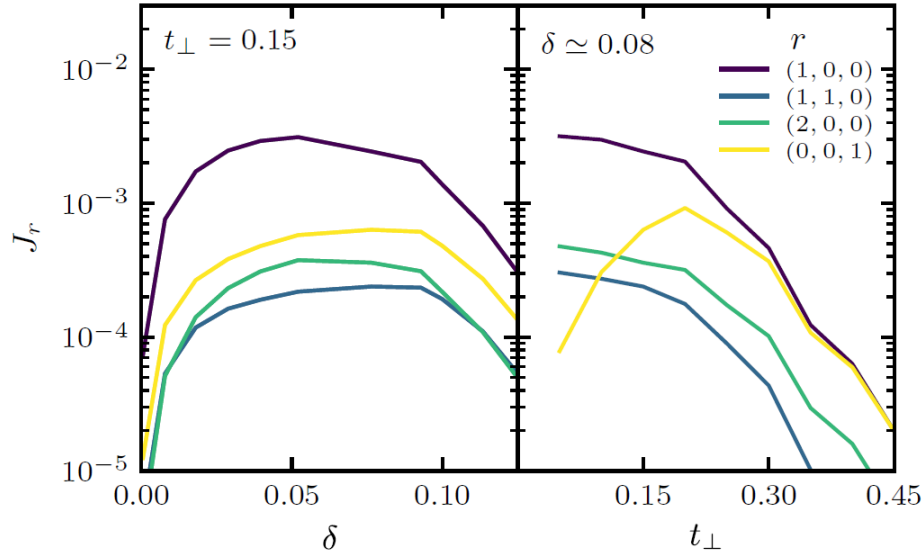


FIG. 2. Josephson coupling J_r as a function of doping δ (left) and interlayer hopping t_{\perp} (right) for different plaquette translations r at $T = 1/52$

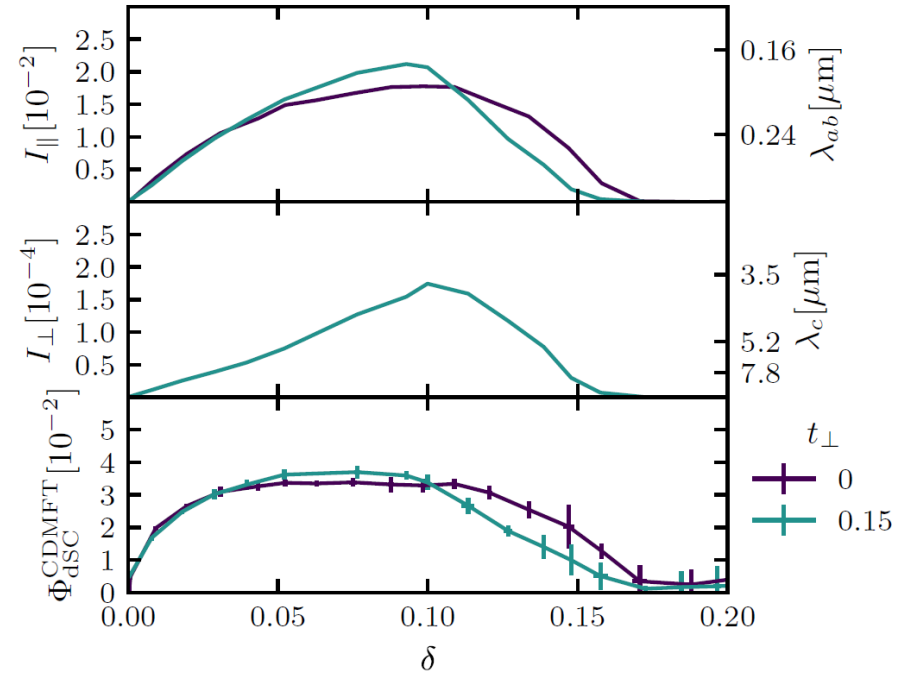
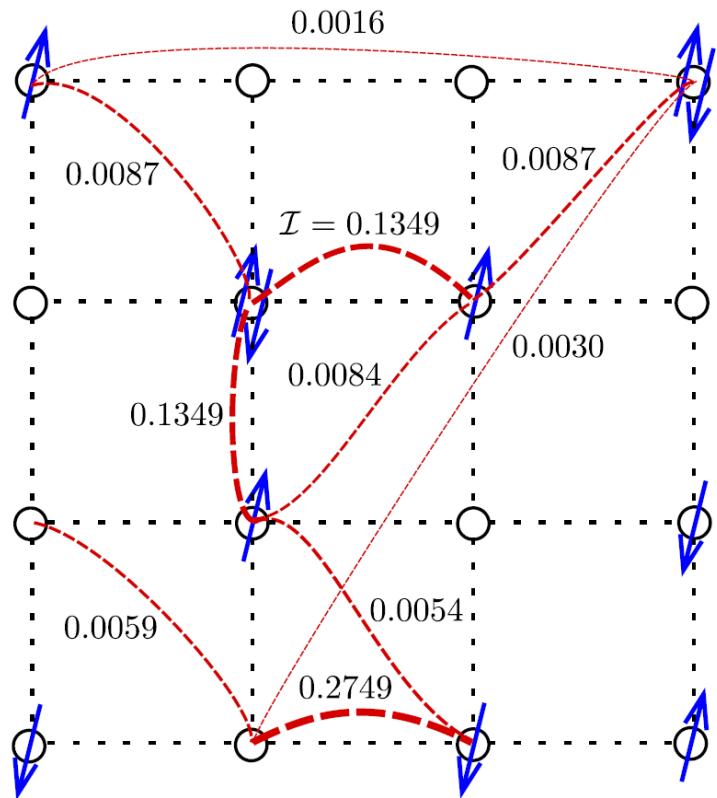


FIG. 5. In-plane superconducting stiffness I_{\parallel} (top, left), in-plane penetration depth λ_{ab} (top, right), perpendicular superconducting stiffness I_{\perp} (center, left), perpendicular penetration depth (center, right), and CDMFT dSC order parameter $\Phi_{\text{dSC}}^{\text{CDMFT}}$ (bottom) as functions of doping δ at $T = 1/52$ for different interlayer hoppings t_{\perp} .

Exact diagonalization for 4 by 4 cluster

A. Bagrov et al, Sci. Rep. (2020) 10:20470

Mutual entropy and information properties of the ground state



Clustering

$$C = \frac{\text{Tr } \mathcal{I}^3}{\sum_{j \neq i}^N \sum_{i=1}^N [\mathcal{I}^2]_{ij}}$$

Disparity

$$Y_i = \frac{\sum_{j=1}^N (\mathcal{I}_{ij})^2}{\left(\sum_{j=1}^N \mathcal{I}_{ij}\right)^2}$$

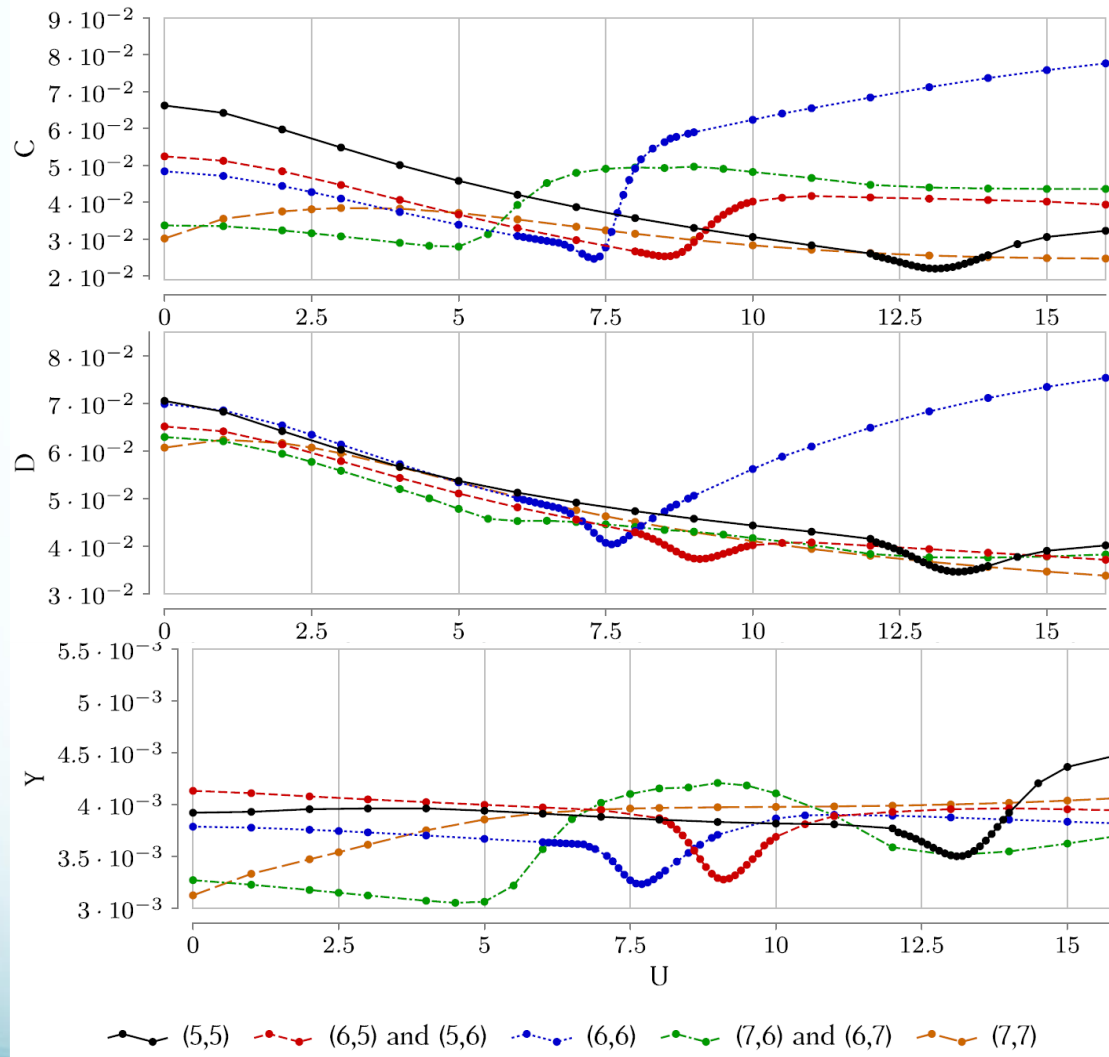
Density

$$D = \frac{1}{N(N-1)} \sum_{i,j=1}^N \mathcal{I}_{ij}$$

Pearson correlations... etc.

Figure 1. An artistic view of the mutual information complex network defined on the Hubbard lattice. While the network is fully connected, for illustrative purposes, only some of the network links are shown. The shown values of inter-site mutual information correspond to the case of non-periodic boundary conditions, (6, 6) sector, $U = 7.5, |t'| = 0.3$. The arrows in the picture are mere for making the idea of a network defined on the Hubbard lattice more graphic and do not reflect any properties of the actual state of the system.

Exact diagonalization for 4 by 4 cluster II



The hopping is $t' = -0.3$, the inverse temperature is $\beta = 100$

Exact diagonalization for 4 by 4 cluster III

Quantum critical point associated to degeneracy can be estimated from quantum information characteristics (as cusp)

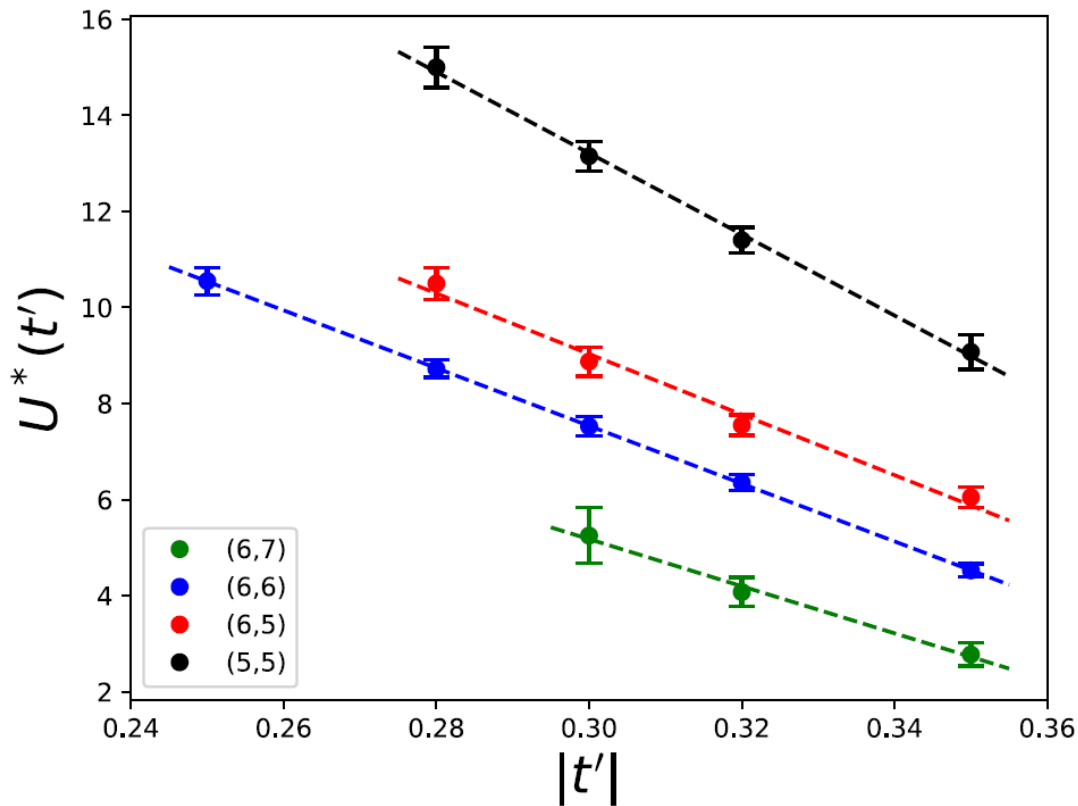


Figure 3. Dependence of the critical Coulomb repulsion U^* on the next-neighbor hopping t' , as the latter is varied in the range $t' \in [-0.35, -0.25]$ for non-periodic boundary conditions at inverse temperature $\beta = 100$. The values are computed as averages of minima of the four complexity measures, and the error bars illustrate the corresponding standard deviations and systematic errors due to the finite step size while scanning over U .

Exact diagonalization for 4 by 4 cluster IV

M. Danilov et al, npj Quant. Mater. (2022) 7:50

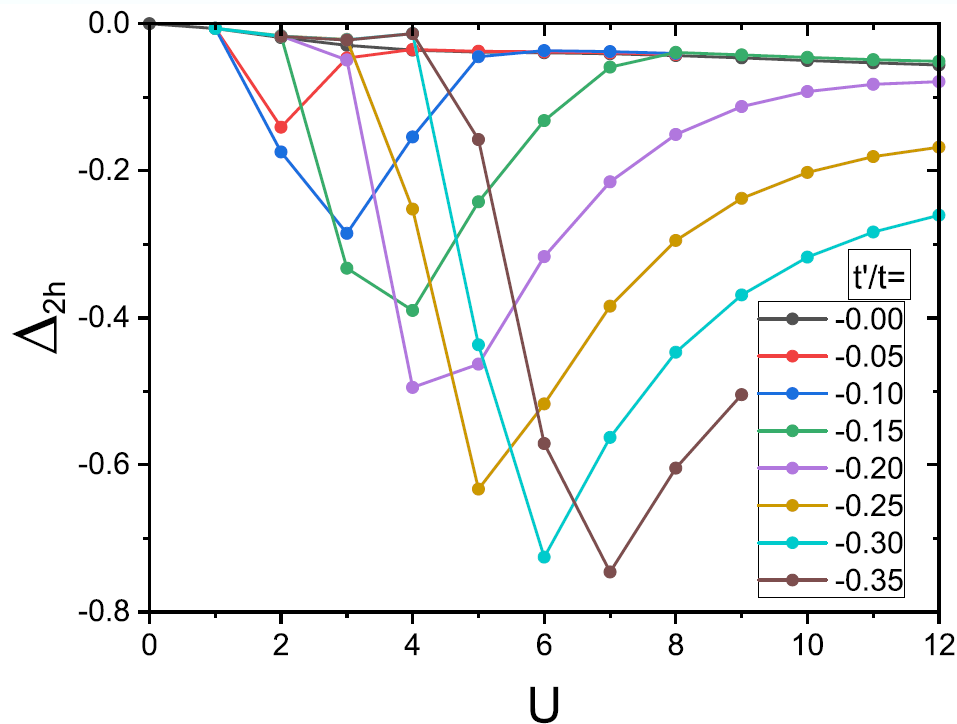


Fig. 2 Hole pairing energy. Pairing energy Δ_{2h} of two holes in a 4×4 cluster with periodic boundary condition as a function of U and t' .

$t = 1$, that is,
0.35 eV

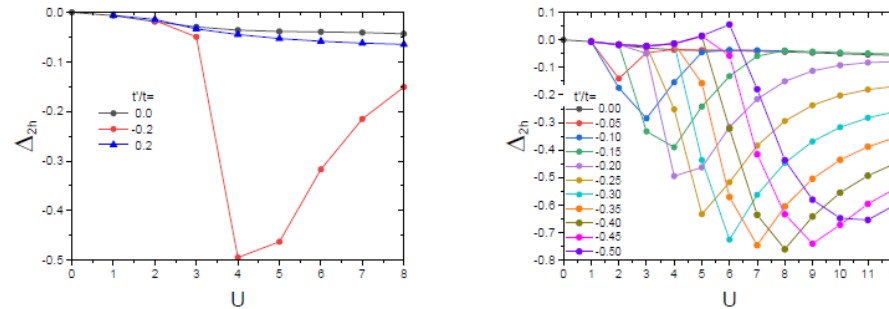
Enormous binding
energy of two holes
at optimal U

Probably the most important result: existence of hole-hole pairs far above T_c
And this is crucially dependent on t' and U ; infinite- U limit (t -J model)
is very different

Exact diagonalization for 4 by 4 cluster V

M. Danilov et al, npj Quant. Mater. (2022) 7:50

The sign of t' is crucially important



Supplementary Figure 8. Energy of two-hole binding for 4x4 periodic cluster for positive, negative and zero values of t'/t as function of U (left) as well as for extended negative values of t'/t (right).

The crucial role of t' in the change of character of magnetic correlations

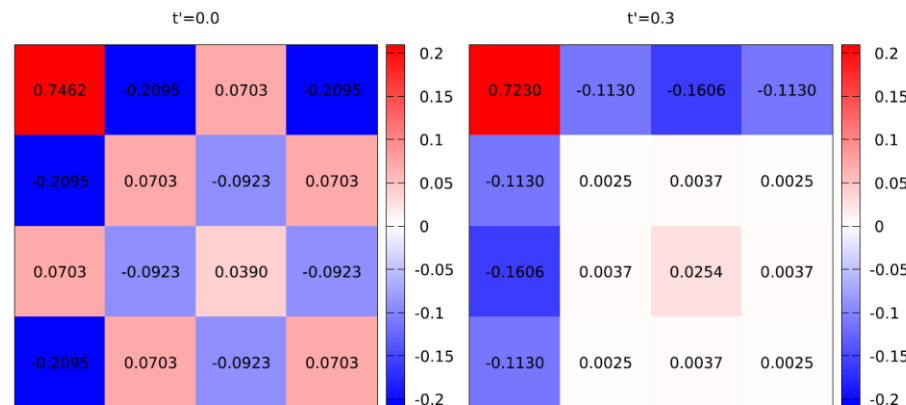


Fig. 3 Spatial spin correlation. Static spin-spin correlation function $\langle M_0 M_l \rangle$ obtained by exact diagonalization for the ground state of the sector $(7\uparrow, 7\downarrow)$ of the 4×4 cluster for $U = 5.56$ and different t' . Whereas $t' = 0$ features clear antiferromagnetic correlations, at $t'/t = -0.3$ these are replaced by stripe-like ferromagnetic correlations. The top-left corner corresponds to $i = (0,0)$.

Exact diagonalization for 4 by 4 cluster VI

M. Danilov et al, npj Quant. Mater. (2022) 7:50

4 by 4 is a minimal size of cluster to catch the effect (as one can see from spatial distribution of the two-hole wave function)

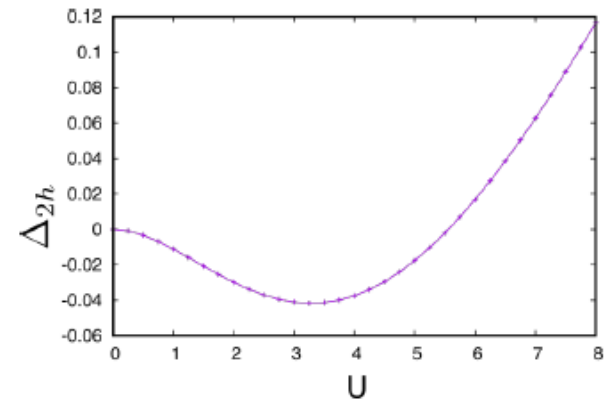


Supplementary Figure 10. Static correlators: $\langle 7 \uparrow, 7 \downarrow | \hat{c}_0^\dagger \hat{c}_j | 7 \uparrow, 7 \downarrow \rangle$ of the (4×4) periodic cluster for $U/t = 5.56$ and $t'/t = 0$ (left) and $t'/t = -0.3$ (right).

What happens in 2 by 2 cluster?

Energy of two-hole binding for 2×2 plaquette for $t'/t = -0.3$.

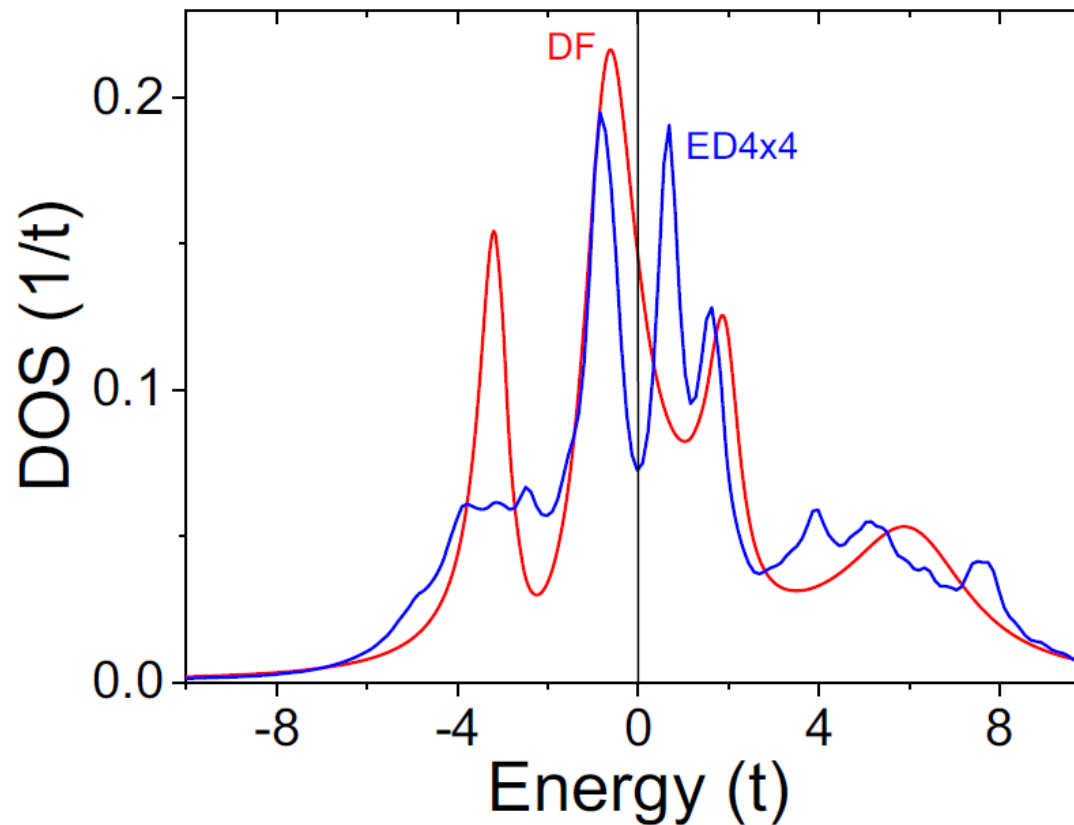
Order of magnitude smaller binding energy



Beyond CDMFT: Dual fermions

M. Danilov et al, npj Quant. Mater. (2022) 7:50

Change of variables in path integral, DMFT is zeroth-order approximation in new variables (Rubtsov, MIK, Lichtenstein 2008)



Pseudogap formation (2nd order perturbative DF)

Conclusions

- Plaquette CDMFT give a simple strong-coupling theory of d-wave superconductivity
- Degenerate plaquette ground state for $x=25\%$ explain main instabilities of d-wave type
- t' is crucially important but only in the context of accidental degeneracy, that is, for moderate U

Many thanks to: Sasha Lichtenstein, Michael Danilov, Viktor Harkov,
Matteo Vandelli, Sergey Brener (Hamburg)
Andrey Bagrov (Nijmegen)
Erik G. C. P. van Loon (Lund)
Sergei Isakov (Michigan)

AND MANY THANKS FOR YOUR ATTENTION